THERMAL MODELING STRATEGIES FOR LASER ASSISTED TAPE WINDING (LATW) PROCESS

S.M. Amin Hosseini[1,2], Ismet Baran[1,3] and Remko Akkerman[1,4]

[1] Faculty of Engineering Technology, Chair of Production Technology, University of Twente, The Netherlands
[2] Email: s.m.a.hosseini@utwente.nl
[3] Email: i.baran@utwente.nl
[4] Email: r.akkerman@utwente.nl

Keywords: Thermoplastic composite, Thermal analysis, Tape winding, Process model, Laser heating

ABSTRACT

The laser assisted tape winding (LATW) is an automated process for manufacturing fibre-reinforced thermoplastic tubular products, such as pipes and pressure vessels. This process consists of several simultaneous physical phenomena including kinematic, optical and thermal behavior. Among these, the in-situ temperature-dependent consolidation of the tapes plays a vital role in the overall quality of the final product. Currently, a new model-based global approach is under development for industrialized production as a part of EU funded Horizon2020 ambliFibre project. There is a need for a highly efficient thermal model to capture the temperature distributions during the process. Therefore, in this study, the capabilities of the various thermal models are evaluated. The actual laser heat flux distribution is estimated from a comprehensive optical model and then subsequently coupled with the thermal model in order to obtain precise temperature distribution. The transient one-dimensional (1D) and 2D models are developed in a Lagrangian framework. The surface boundary conditions are moving with winding velocity and the mesh remains stationary. The transient approach is used by conventional finite volume (FV) method. The hoop winding process is quantified for various winding speeds using coupled optical-thermal models which have never been done up to now. Since the real LATW process includes many considerations that disturb the spatial temperature field, e.g., various winding angle and non-uniform laser heat influx, a 2D transient model is, therefore, convenient for the LATW process simulation. However, for hoop winding the 1D model is almost as accurate as the 2D model and less computationally expensive. The history of nip point temperature for 10 layers of the continues hoop winding is predicted. Also, the peak in the nip point temperature history which is a physical phenomenon taking place during the LATW process is explained.

1 INTRODUCTION

There is an increasing demand for fibre-reinforced plastic (FRP) composite components having a high strength-to-weight ratio. Tubular structures constitute a major share of FRP components in various applications including pipes, tanks, transportation, wind energy and construction industry. An emerging sub-group of these products uses thermoplastic polymers as the matrix, which makes production processes faster with lower energy consumption that is not available with the commonly used thermoset. The LATW is an automated process in which tubular parts are built up layer-by-layer onto a winding mandrel or a liner, a thermoplastic diffusion barrier, using a modular tape winding unit controlled robotically. The process is based on the winding of tapes that consist of continuous unidirectional fibers embedded into a solidified thermoplastic matrix terms pre-preg. The incoming pre-preg tape and the already laid down tape, terms substrate, are locally molten by the absorption of laser radiation before touching each other (at the so-called nip-point) as seen in Fig. 1. The in-process consolidation of the molten tapes leads to bonded fiber-reinforced thermoplastic layers.

Within EU-funded HORIZON2020 "ambliFibre" project the first intelligent model-based controlled LATW system for thermoplastic FRP components will be developed and validated. A virtual process model facilitates fast adaptation with varying product requirements, waste reduced production, and higher reliability of system and product. Additionally, this model provides information about arising failures of the product which in turn avoid the expensive trial-and-error approaches [1].

Among various phenomenon accruing simultaneously, the thermal analysis receives much attention from literature [2–13], since other parameters are highly dependent on temperature distribution, e.g., interface bond strength, crystallinity, and thermal residual stresses. However, a comparative study to assess the capabilities of thermal models is missing in the literature specifically for the LATW process. By doing so, a comprehensive overview will be gained to predict the temperature in various phases of the LATW process by an efficient model. The present work considers the global domain including the nip point region for a hoop winding (90°) process.

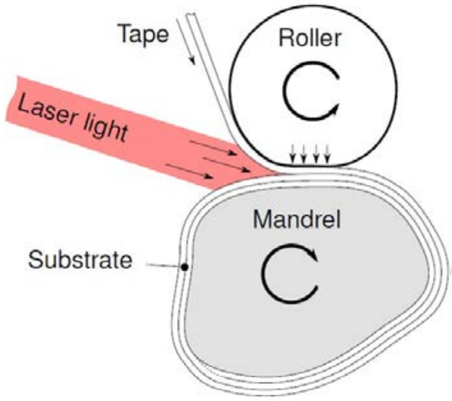

Figure 1: Schematic side view of LATW process.

2 COUPLED THERMAL-OPTICAL MODEL

The material is carbon-reinforced PEEK, the power of the laser is 450 W with a top-hat distribution. Table 1 provides a listing of model parameters that are used for simulation.

Parameter	*Value [Unit]*
Transverse thermal conductivity of tape (though-thickness)	0.72 [W/(m K)]
Longitudinal thermal conductivity of tape (in-fibre direction)	5 [W/(m K)]
Tape density	1560 [kg/m^3]
Tape specific heat	1425 [J/(kg K)]
Environment / initial temperature	293 [K]
Tape-air heat transfer coefficient	10 [W/(m^2 K)]
Substrate-tool heat transfer coefficient	500 [W/(m^2 K)]
Tape emissivity	0.9
Nodes per tape(through-thickness)	2
Placement velocity	various [mm/sec]
Laser intensity	1461 [W/mm^2]

Table 1: Overview of thermal model parameters and process settings used for simulation

The domain of the problem includes a thermoplastic ring consisting of previously laid down substrates. The plane perpendicular to the ring surface and at the middle of the tape width is considered as the 2D computational domain. Multiple 1D through-thickness domains within the 2D domain are created. A definition of the problem is demonstrated in Fig. 2. The cylindrical ring is mapped to the Cartesian coordinate system without losing accuracy. The boundary conditions at the top surface are time-dependent. In Fig. 2b, the effect of growing thickness of the ring is considered while in Fig. 2a only the laser heat flux is shown. The temperature of the nip point is estimated by averaging the temperature of the incoming tape and the calculated temperature of the substrate at the location of the nip point as done in [14,15].

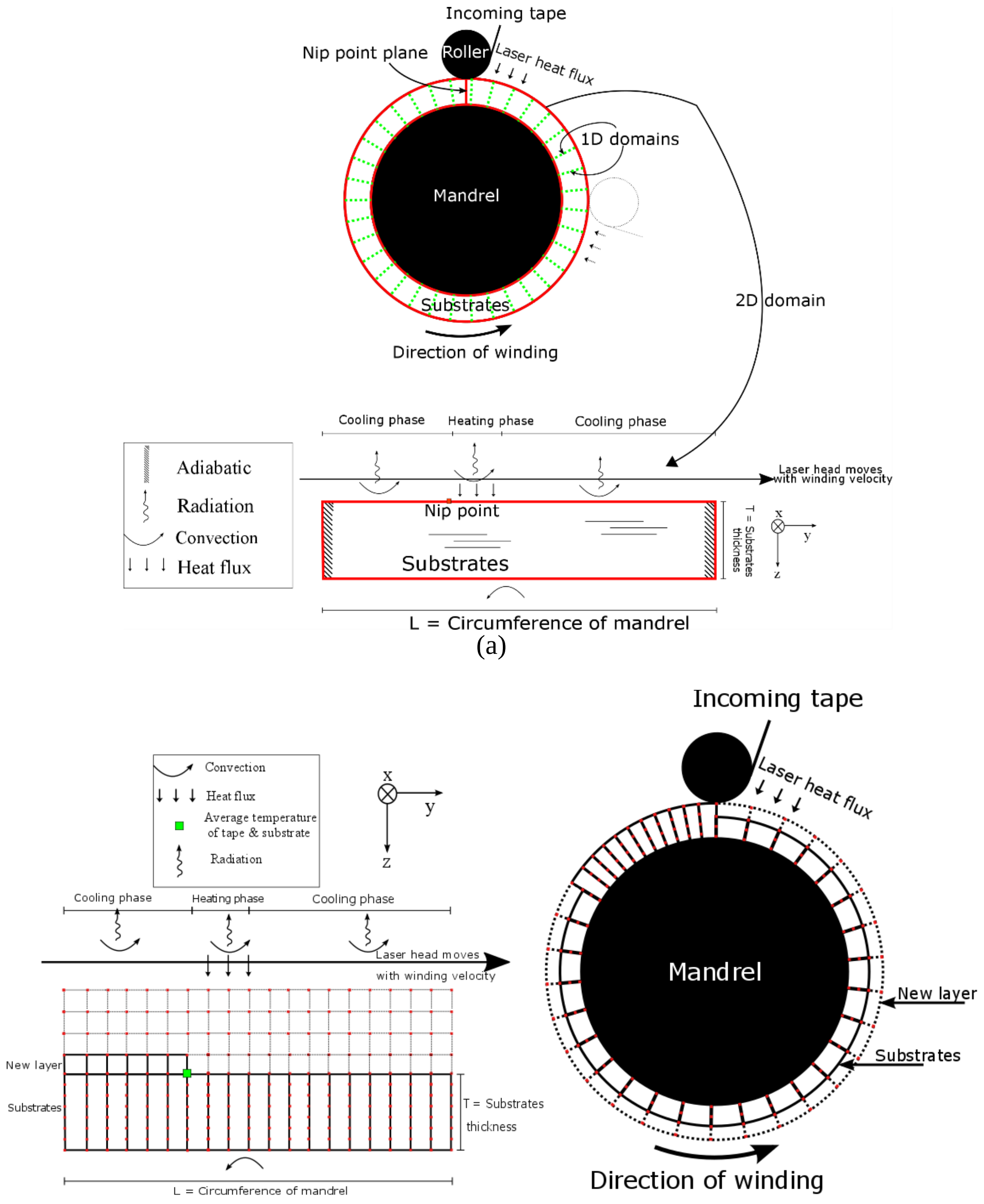

(b)

Figure 2: Schematic view of the 1D and 2D heat transfer problem for the LATW process (a) neglecting the effect of growing thickness, (b) including the effect of growing thickness.

The heat flux distribution on the surface of the substrate is based on a ray tracing approach (Fig. 3) [2]. To model the anisotropic reflective behavior of composite surface, a non-specular reflection model is implemented, using a bidirectional reflectance distribution function (BRDF) which was developed by Reichardt et al. [15]. It is seen from Fig. 3 that the heat flux is close to 0 near the nip point due to the shadowing effect, i.e. the laser beam cannot reach nip point due to the geometry. It should be noted that the heat flux covers 46 mm region in front of the nip point. The scattering behavior of the heat flux distribution is mainly due to cylinder-like carbon fibers on the composite surface that reflect light in multiple directions. Also, the surface roughness of the tape is a source for scattered heat distribution which is well predicted by BRDF model.

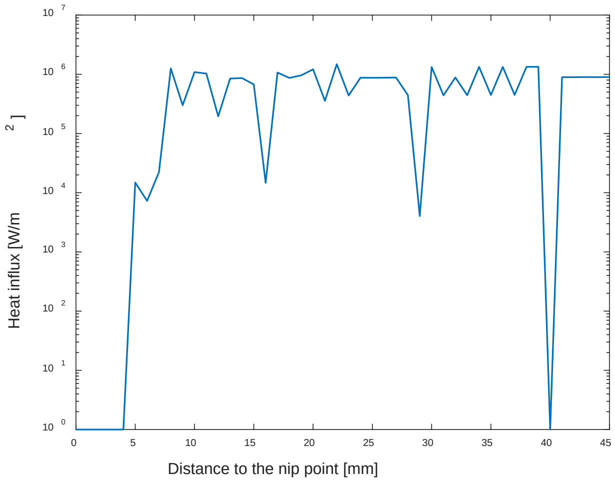

Figure 3. Heat influx from laser source extracted from the optical model. It is distributed on the substrate surface starting from nip point (0 on the x-axis).

The governing heat transfer equations for 1D and 2D domains in the Lagrangian framework are written in Eq. 1 and 2, respectively:

$$\frac{\partial T}{\partial t} = \alpha\left(\frac{\partial^2 T}{\partial z^2}\right) + q'' \tag{1}$$

$$\frac{\partial T}{\partial t} = \alpha\left(\frac{\partial^2 T}{\partial y^2} + \frac{\partial^2 T}{\partial z^2}\right) + q'' \tag{2}$$

An explicit FD method is used to solve the 2D and 1D heat transfer equations. In the Lagrangian framework, the boundary conditions are time-dependent which considers the effect of velocity.

For tape placement process, the profile of laser intensity is evenly distributed across the laser spot width which is larger than the tape width. Therefore, it is possible to assume uniform temperature distribution for the incoming tape and substrate in width direction. On the other hand, the heat conduction rate is much lower than the rate at which the laser head moves, and it is therefore assumed that the in-plane conduction could be neglected as suggested also in [2]. Consequently, a 1D transient through-the-thickness model is implemented. Due to the rotating behavior of LATW process, heat input to the incoming substrate is transferred to the location where it starts to propagate earlier. So, it seems that this assumption is not valid for the LATW process. By considering the in-plane conductivity a 2D model is developed.

3 RESULTS AND DISCUSSION

A contour plot of the temperature distribution in the 2D domain is presented during the process in Fig. 4. The predicted temperature by 1D and 2D model is found to be almost the same with winding speeds larger than 100 mm/s and a maximum of 10°C difference is noticed at a winding speed of 10 mm/s. As a result, the 1D model can be considered as accurate as the 2D model for hoop winding process. At lower velocities, the in-plane conduction effect is more effective. As the velocity increases, this difference approaches zero as expected. The 1D model predicts higher temperatures in the global domain. The reason is that the input heat from laser does not dissipate in the longitudinal direction and accumulated in the location of the 1D domain which can be considered as an insulated domain.

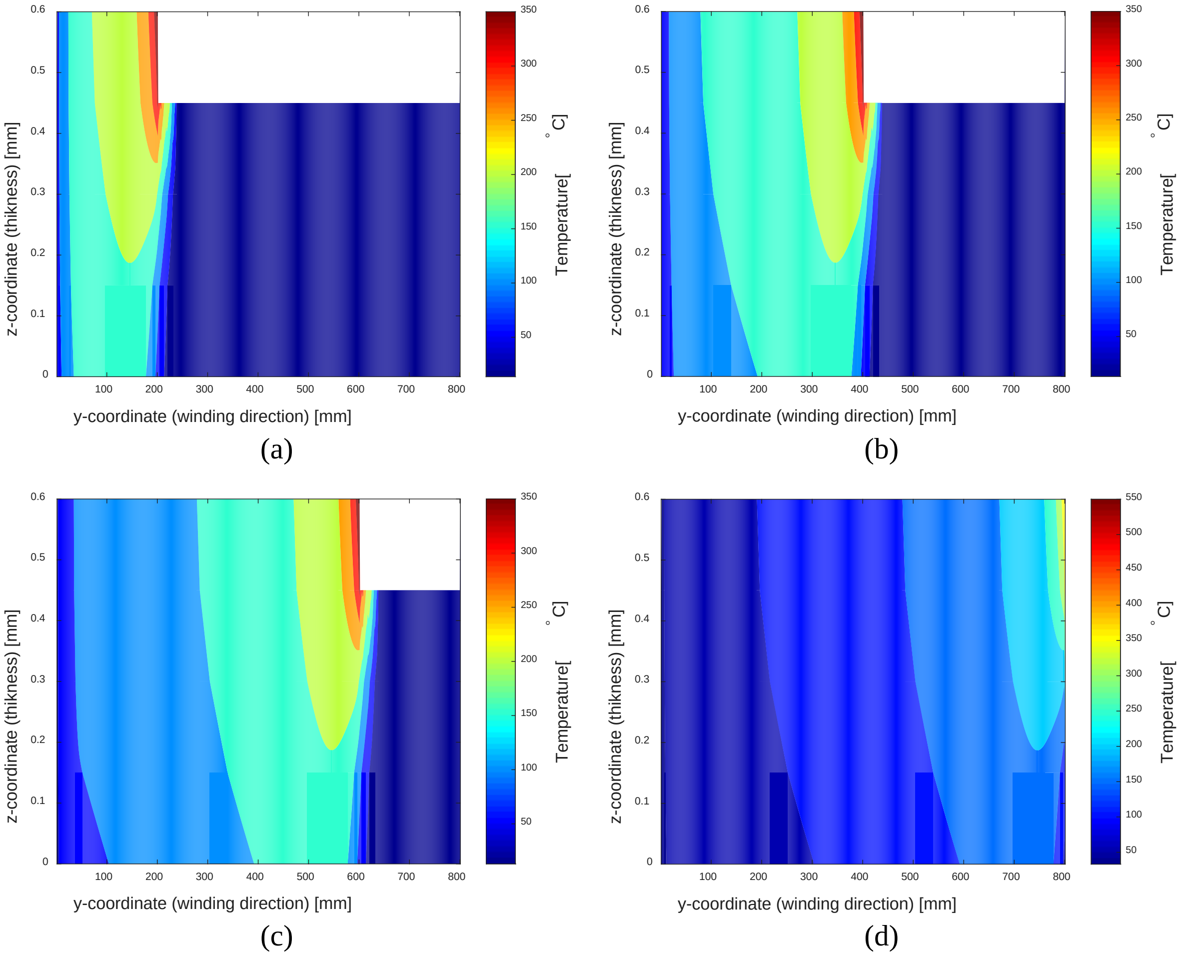

Figure 4: Temperatures distribution contour in the 2D domain during the process at (a) ¼, (b) ½, (c) ¾, and (d) end of the process time. 3 layer is placed already as substrate. A new layer is placed on the third layer with the velocity of 200mm/sec.

The nip point temperature needs some time to reach a constant value (steady-state phase) when the laser head starts moving. For various velocities, this time changes together with the value of the nip point temperature as seen in Fig. 5. According to Table 2, the distance which is required to reach steady-state phase is the same, therefore, this parameter is independent of the velocity. It mainly depends on the height of the laser spot and heat conductivity through the thickness. It could be concluded that within this distance extra laser power is needed to compensate for the nip point temperature to ensure proper bonding of the layers. This can be considered as the case for the very first layer laid down onto a thermoplastic liner for the LATW process. The increase in speed causes the decrease in nip point temperature as expected. The laser power should be increased to have a steady-state temperature at least higher than the processing temperature of PEEK polymer which has a melting point of 343°C.

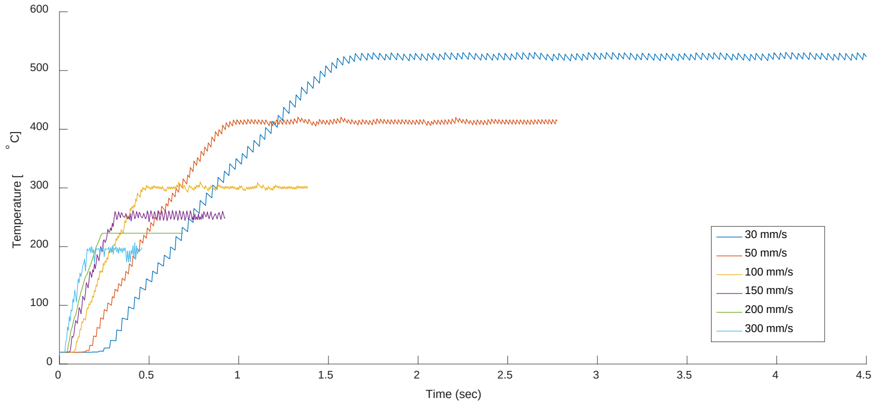

Figure 5: Predicted nip point temperature history for 150 mm movement of the laser head on the substrate.

Velocity (mm/s)	30	50	100	150	200	300
Time to steady-state phase (s)	1.67	0.98	0.48	0.31	0.23	0.15
Distance to steady-state phase (mm)	50.1	49	48	46.5	46	45
Steady-state temperature (s)	523	414	301	253	223	193

Table 2. Effect of velocity on the parameters related to nip point.

A noisy behavior of the nip point temperature history is seen in Fig. 5. The mesh size on the top surface is 1 mm in the y-direction, i.e., node-1 equals to 0 mm, node-2 equals to 1 mm and so on. Depending on the size of the time step and the winding velocity, the laser head moves with different amount of distance in each time step. It is assumed that the real location of the laser head, rounded to the nearest nodes of the surface in the computational domain where the heat transfer equation is solved. In the Fig. 6, the head stays at node-3 for four time steps while at node-1 stays just one time step. Therefore, the laser head does not move evenly during the time in the computational domain. Moreover, during the time steps that the laser head is stationary, the nip point loses heat which is not physically true since the laser head moves continuously.

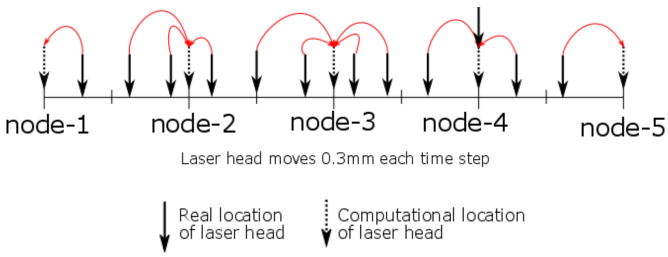

Figure 6: Location of nip point in real time and in discretized domain

The temperature of the nip point and the substrate was measured online by the infra-red (IR) camera and reported in experiments by [14]. The measurements are depicted in Fig. 7. The location where the temperature was recorded is shown in Fig. 7c. During winding a specific layer the nip point temperature is almost steady as can be seen in Fig. 7a at the time approximately from 11 s to 12 s.

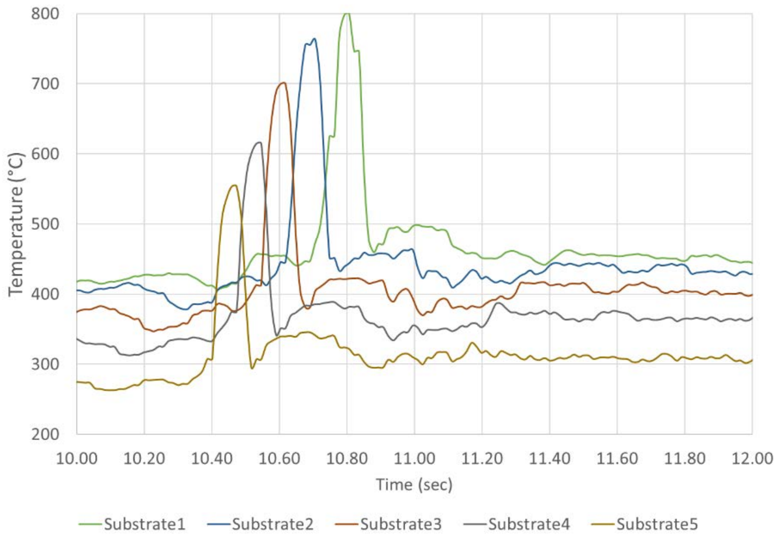

(a)

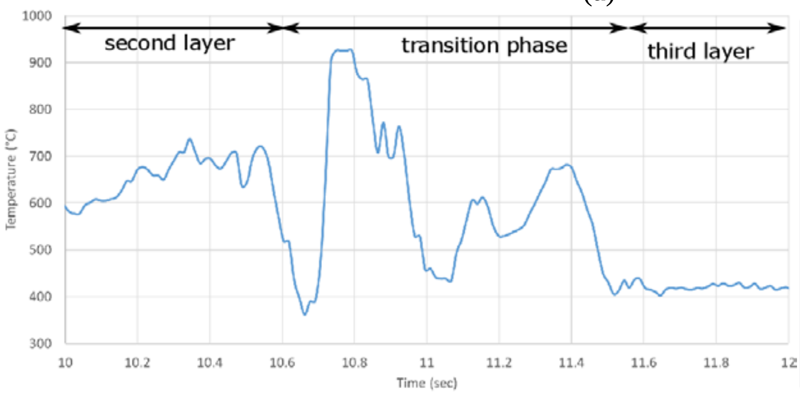

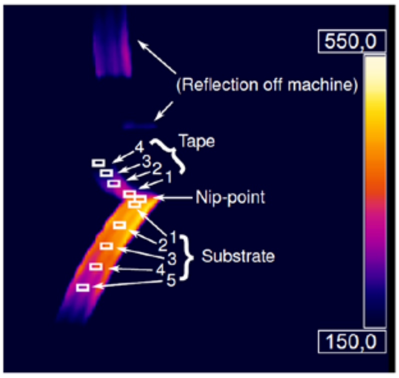

(b) (c)

Figure 7. Temperature measured by an IR camera for a LATW process with the velocity of 100 mm/sec and mandrel diameter of 244 mm, when (a) layer 15 is placed on the layer 14 (b) layer 3 is placed on the layer 2 with the same setting of the process. (c) locations where the temperature is recorded by the thermal camera.

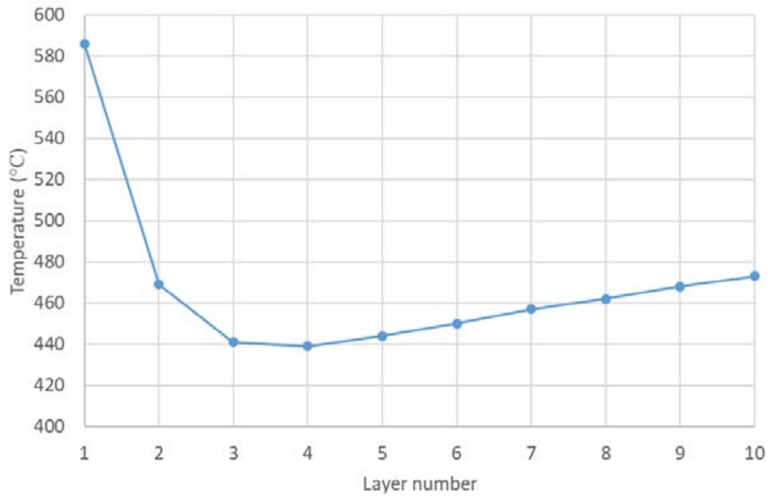

Figure 8. Predicted temperature history of the nip point at steady state phase during winding 10 layers

The temperature at steady state phase for each layer during winding of 10 layers is shown in Fig. 8. One layer is assumed as the substrate. At lower layer number, the steady state temperature would decrease as a new layer is added. The nip point temperature drops from 586°C to 469°C when layer 2 is added on top of layer 1. This phenomenon is also observable in Fig. 7b where there is a decrease when the 3rd layer is wounded over the 2nd layer (considering second 10 and 12). The amount of heat influx from the laser and incoming tape temperature (400°C) is fixed while the amount of material is increased on the substrate, i.e. growing layers. Hence, more material on the substrate should be heated by the laser which results in a lower temperature of the substrate. Moreover, the temperature of the tape is much lower than the 1st layer nip point temperature. So, after the consolidation of tape and substrate where the temperature is averaged, the nip point temperature reduces. This trend exists until 4th layer as seen with the predictions in Fig. 6. After winding of 4th layer, the nip point temperature increases slightly (6°C per layer). This increase is also validated by measurements presented in Fig. 7a which is around 20°C. The reason for the difference between the predicted and measured temperature could be related to the thermal resistance between the top surface and mandrel which acts as a heat sink. As more material is added to the substrate the thermal resistance becomes higher and less heat dissipated to the mandrel. Therefore, the heat is accumulated in the substrate and the temperature increases. Depending on the winding velocity, the layer where the nip point temperature starts increasing changes accordingly. For instance, at 200 mm/sec winding speed, after the 2nd layer is laid down, the nip point temperature starts increasing (it was after 4th layer with 100 mm/s winding speed) since the material has less time to cool down during winding.

When a new layer is placed on the previously laid down layer, the IR camera measures a peak in the temperature as depicted in Fig. 7a,b at 10.8 seconds. The observed peak in the nip point temperature when a new layer is placed needs more discussion. Many effects may involve in this phenomenon. A brief but intense overheating ay the initiation of the winding process is observed in tests done in [14]. This overheating may induce the degradation of the material and therefore a deconsolidation of the polymer may happen. However, to explain this phenomenon the same approach seen in Fig. 2a is assumed with a slightly change in the geometry that is demonstrated in Fig. 9. The fiber direction is in the y-direction. The bump is considered as the representative of the previously placed tape which has a larger thickness. Actually, a bump as a geometrical discontinuity is assumed in the way of heating region movement. The model simulates the effect of this geometry change, i.e. growing layer for the substrate, on the thermal field. At the edges of the bump, convection boundary condition is defined. The length of the domain is 760 mm (the circumference of the mandrel). The laser head starts moving 100 mm before the bump and 100 mm after it with the velocity of 100 mm/sec.

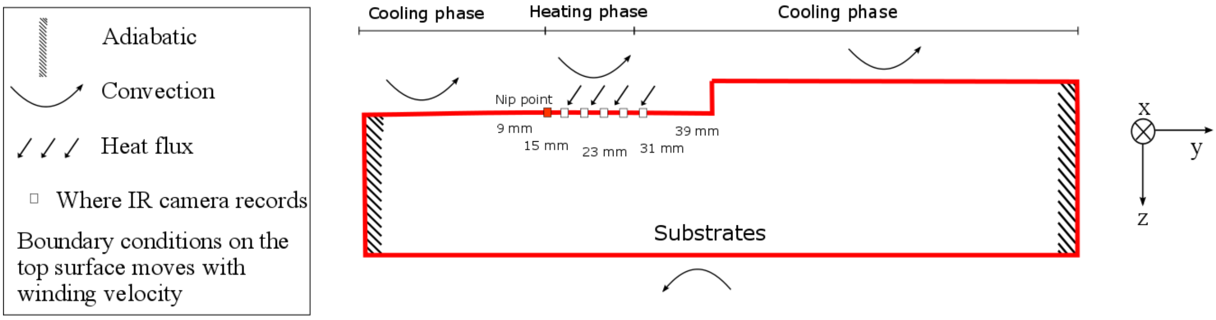

Figure 9. Schematic view to study the peak in temperature evolution of the nip point.

The predicted temperature of the various points with specified distance before the nip point is shown in Fig. 10. As mentioned, the heat flux covers 45 mm region in front of the nip point and the maximum peak temperature is obtained at a location 9 mm before the nip point. The maximum peak temperature gets lower at nodes more away from the nip point as expected. The reason is that the nodes closer to the nip point are more exposed to the heating region and therefore receives more heat comparing the nodes far from the nip point. Considering the trend of the nip point temperature history, the predicted peak by the model agree well to measured temperature in Fig. 7a. However, the values of the predicted peaks are lower than measurements. If the bump is neglected, then the peaks are not noticed anymore. So, this geometrical change on the surface could be introduced as one of the effects for the peak observed during the winding process. A more accurate simulation model to predict the value of the peaks compared with the experimental measurements is required. Change in the thermal properties of the polymer due to deconsolidation or change in the reflection behavior of the laser light is suggested as improvements for the modified model.

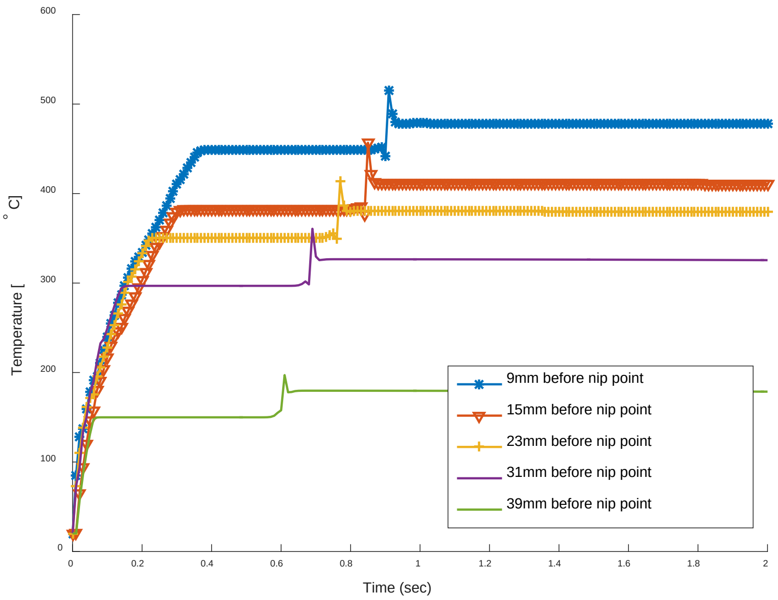

Figure 10. Temperature history of the points before nip point when layer 15 is placed on the layer 14 (refer to Fig. 7c and Fig. 8 for the location of the points).

4 CONCLUSIONS

In this study, the capabilities of the transient thermal models in the Lagrangian frame is evaluated. For the LATW process, the simplest model including the effects of in-plane conduction is a transient 2D model. The 2D model is capable of explaining the temperature change in the nip point during winding. Also, the peak temperature at nip point recorded by IR camera is explained. The change in the geometry of the surface is considered as one of the effects that induce the peak in the temperature. Moreover, it should be taken into account that the nip point needs some time to reach to its presumed temperature for proper bonding between layers and therefore more power is required when the laser head starts moving in every winding step. As a result, the 2D transient model would be appropriate for process simulation. However, the 1D model is also efficient to predict the temperature for hoop winding and can be used to reduce computational cost.

Future work will focus on validating the developed model experimentally for different lay-up of the tape and substrate. Therefore, the effect of conduction in a 3D domain could be investigated.

ACKNOWLEDGEMENTS

This work is done within the ambliFibre project. This project has received funding from the European Union's Horizon 2020 research and innovation program under grant agreement No. 678875.

REFERENCES

[1] European Commission. adaptive model-based control for laser-assisted fibre-reinforced tape winding.
[2] W. Grouve, Weld Strength of Laser-Assisted Tape-Placed Thermoplastic Composites, PhD thesis, University of Twente, 2012. (doi:10.3990/1.9789036533928.)
[3] X. Wang, D.Y.S. Lou, Simple thermal model for online laser curing of thermoset composites in filament winding, *International Journal of Energy Research*, **27,** 2003, pp. 377–388. (doi:10.1002/er.882.)

[4] S.C. Dai, L. Ye, Characteristics of CF/PEI tape winding process with on-line consolidation, *Composites Part A: Applied Science and Manufacturing*, **33**, 2002, pp. 1227–1238. (doi:10.1016/S1359-835X(02)00083-0.)

[5] B. Chern, T.J. Moon, J.R. Howell, Thermal Analysis of In-Situ Curing for Thermoset, Hoop-Wound Structures Using Infrared Heating: Part I—Predictions Assuming Independent Scattering, *Journal of Heat Transfer*, **117**, 1995, 674. (doi:10.1115/1.2822629.)

[6] L. Zhao, S.C. Mantell, D. Cohen, R. Mcpeak, Finite element modeling of the filament winding process, *Composite Structures*, **52**, 2001, pp. 499–510.

[7] C.M. Stokes-Griffin, P. Compston, T.I. Matuszyk, M.J. Cardew-Hall, Thermal modelling of the laser-assisted thermoplastic tape placement process, *Journal of Thermoplastic Composite Materials*. **28**, 2013, pp. 1445–1462. (doi:10.1177/0892705713513285.)

[8] J. Kim, T.J. Moon, J.R. Howell, Transient Thermal Modeling of In-Situ Curing During Tape Winding of Composite Cylinders, *Journal of Heat Transfer*, **125**, 2003, 137. (doi:10.1115/1.1527912.)

[9] A. Hajiloo, W. Xie, S. V. Hoa, S. Khan, Thermal control design for an automated fiber placement machine, *Science and Engineering of Composite Materials*, **21**, 2014, pp. 427–434. (doi:10.1515/secm-2013-0009.)

[10] M. Tannous, A. Barasinski, C. Binetruy, B. Courtemanche, Contribution of thermo-mechanical parameters and friction to the bonding of thermoplastic tapes in the tape winding process, *Journal of Materials Processing Technology*, **229**, 2016, pp. 587–595. (doi:10.1016/j.jmatprotec.2015.10.013.)

[11] Y.M.P. Toso, P. Ermanni, D. Poulikakos, Thermal phenomena in fiber-reinforced thermoplastic tape winding process: Computational simulations and experimental validations, *Journal of Composite Materials*, **38**, 2004, pp. 107–135. (doi:10.1177/0021998304038651.)

[12] N. Hassan, A Heat Transfer Analysis of the Fiber Placement Composite Manufacturing Process, *Journal of Reinforced Plastics and Composites*, **24**, 2005, pp. 869–888. (doi:10.1177/0731684405047773.)

[13] A. Zaami, I. Baran, R. Akkerman, Numerical Modelling of Laser Assisted Tape Winding Process, *20th International ESAFORM Conference on Material Forming, Ireland, 2017.*

[14] J.M. Reichardt, Optical-Thermal Process Model for Laser-Assisted Tape Winding, Master thesis, University of Twente, 2016.

[15] J.M. Reichardt, I. Baran, R. Akkerman, Optical Process Model For Laser-Assisted Tape Winding, *ECCM17 - 17th European Conference on Composite Materials, Munich, Germany 2016.*